Surface magnetism studied within the mean-field approximation of the Hubbard model

M. Potthoff and W. Nolting
Humboldt-Universität zu Berlin, Institut für Physik, Invalidenstrasse 110, 10115 Berlin, Germany
(Received 18 May 1995)

Collective surface magnetism is studied within the mean-field approximation of the semi-infinite Hubbard model for the (100) surface of a simple cubic lattice. We investigate the changes of electronic and related magnetic properties at the surface with respect to the bulk that are introduced due to the reduction of the coordination number of atoms at the surface. Using a standard recursion method, the equation of motion for the one-electron Green function is solved numerically yielding the spin- and layer-dependent local density of states (LDOS). From this the layer-dependent charge density and magnetization are derived self-consistently. The LDOS of the first few layers below the surface clearly deviates from the bulk density of states which results in strong changes of the layer magnetizations while charge-transfer effects may be rather small. We systematically investigate the dependence of the layer magnetization on the Coulomb interaction, the band filling, and the temperature for the ferromagnetic as well as for different antiferromagnetic structures. While for the antiferromagnetic solutions the (sublattice) magnetization of the topmost layer is always enhanced, a higher magnetization of the topmost layer is only found for not too strong Coulomb interaction in the case of the ferromagnet. In the fully polarized ferromagnetic state the magnetization is dominated by the charge transfer between the bulk and the surface. First-order transitions from the ferromagnetic to a layerwise antiferromagnetic phase are studied in detail. Metastable ferromagnetic solutions are found beyond the critical point (Coulomb interaction, temperature). The actual transition of the metastable ferromagnetic into the stable antiferromagnetic phase starts from the very surface, which acts as an immanent perturbation of the infinitely periodic lattice. The antiferromagnetic order quickly extends into the bulk layer by layer.

I. INTRODUCTION

Electronic and related magnetic properties at the surfaces of band magnets are an important subject of present research.[1–10] For band ferro- and antiferromagnets the magnetization derives from itinerant valence electrons. The itinerant nature of the valence electrons causes the magnetic properties to be a sensitive function of local environment. Consequently, the magnetism of a band magnet is strongly affected by the lattice structure.[11,12] An even more pronounced effect of the local geometry on the magnetic properties is to be expected at the crystal surface. The absence of some neighbors of atoms at the surface should cause considerable changes in the local magnetic properties.

Such varied behavior can be studied within the mean-field approximation of the semi-infinite Hubbard model. Conventionally, the Hubbard model[13–15] applies to correlated electrons moving through a strictly periodic and infinitely extended lattice. To deal with surface effects, however, a semi-infinite system of lattice sites should be considered. The resulting "semi-infinite Hubbard model" differs from the usual three-dimensional Hubbard model only with respect to the purely geometrical cutoff of the nearest-neighbor hopping at the surface. Opposed to Heisenberg-type models, its main advantage to investigate itinerant magnetism rests on the fact that the magnetic properties can be derived consistently from the underlying electronic structure.

To simplify the related many-body problem to a tractable form, we apply the mean-field (Hartree-Fock) approximation. This guarantees the model to be numerically solvable, while the Coulomb interaction is retained in the most simple way. Despite its crudeness, the mean-field approximation is interesting of its own, since in most band-structure calculations based on density-functional theory and the local-density approximation, band magnetism is described in a way that more or less corresponds to the mean-field approach. In some recent work the mean-field approximation is even implemented explicitly to deal with surface magnetism.[6–10] The results obtained for Cr, Fe, and Ni surfaces at zero temperature indeed agree reasonably with experiments.

The model surface we consider represents a highly idealized subject for investigating the local magnetic properties. This is not only due to the simplicity of the Hubbard model itself and due to the mean-field approximation but also due to the neglect of effects on the electronic parameters that enter the Hubbard model. At the very surface the hopping integrals T_{ij} and also the Coulomb interaction U may differ significantly from their bulk values. Such and other effects, however, are assumed to be of less importance; the semi-infinite Hubbard model focuses on the most important point in the context of itinerant surface magnetism: the reduction of the coordination number of atoms at the surface.

The main purpose of this paper is not to present results to be compared with experimental findings directly. Instead, we aim at a systematic study to look for qualitative new effects and to show up general dependencies of the local magnetic properties at the surface on the essential model parameters: the Coulomb interaction U, the band filling $\langle n \rangle$, and the temperature T. Such trends may be of particular importance in the understanding of surface magnetism. Simple tight-binding models are well known to be rather successful in reproducing the qualitative dependencies of surface-related quantities on geometric as well as electronic parameters.[1] Up

0163-1829/95/52(21)/15341(14)/$06.00

to now, however, little is known about surface magnetism within the semi-infinite Hubbard model.

We have chosen the (100) surface of a simple cubic crystal as the model surface for our present study. The magnetization for each layer parallel to the surface is calculated from the spin-dependent local occupation numbers, which are determined self-consistently from the spin- and layer-dependent local density of states (LDOS). The LDOS is calculated by means of the recursion method[16,17] at all nonequivalent sites of the semi-infinite system. We consider systematically the dependencies on U, $\langle n \rangle$, and T for the paramagnetic, the ferromagnetic and for different antiferromagnetic phases. The stability of the solutions and the order of transitions between the different phases is derived from the internal energy or, at $T>0$, the free energy.

The following section briefly introduces the key quantities of the theory. Sections III and IV sketch the way the theory is evaluated numerically. The presentation and interpretation of the results is devoted to Sec. V. It includes the discussion of the bulk phase diagram (Sec. V A) and of the spin- and layer-dependent LDOS at the crystal surface (Sec. V B). The layer magnetization and its dependencies on the strength of the Coulomb interaction and on the band filling as well as the role of the surface for phase transitions are discussed in detail in Sec. V C. We then turn to the temperature dependence of the layer magnetization (Sec. V D). Finally, in Sec. VI we summarize the main results and give some concluding remarks.

II. THEORY

We consider itinerant electrons in a narrow nondegenerate energy band described within the framework of the Hubbard model:

$$H = \sum_{ij\sigma} (T_{ij} - \mu\delta_{ij}) c_{i\sigma}^{\dagger} c_{j\sigma} + \frac{1}{2} U \sum_{i\sigma} n_{i\sigma} n_{i-\sigma} . \quad (1)$$

$c^{\dagger}$ (c) is the creation (annihilation) operator for a valence-band electron, which is specified by the lower indices: $\sigma = \uparrow, \downarrow$ is the index of electron spin; i and j are assumed to refer to the sites of a semi-infinite lattice. Thereby, the Hamiltonian allows for the description of the crystal surface which we choose to be the (100) surface of a simple cubic crystal. T_{ij} denote the hopping integrals. In the bulk they are related to the Bloch energies $\epsilon(\mathbf{k})$ via

$$T_{ij} = \frac{1}{N} \sum_{\mathbf{k}} e^{i\mathbf{k}(\mathbf{R}_i - \mathbf{R}_j)} \epsilon(\mathbf{k}) . \quad (2)$$

At the surface the hopping integrals are assumed to remain unchanged. The electronic and magnetic structure at the surface are expected to be decisively influenced by the reduction of the coordination number from $z_1^{(B)} = 6$ in the bulk to $z_1^{(S)} = 5$ for atoms in the topmost surface layer. Further important model parameters are the intra-atomic Coulomb interaction U and the width of the free Bloch band W. μ stands for the chemical potential, and $n_{i\sigma} = c_{i\sigma}^{\dagger} c_{i\sigma}$ is the occupation-number operator.

All interesting one-particle properties of the system are determined by the retarded one-electron Green function,

$$G_{ij\sigma}(E) = \langle\langle c_{i\sigma} ; c_{j\sigma}^{\dagger} \rangle\rangle_E^{\mathrm{ret}} , \quad (3)$$

or, equivalently, by the corresponding one-electron spectral density,

$$A_{ij\sigma}(E) = -\frac{1}{\pi} \mathrm{Im}\, G_{ij\sigma}(E) . \quad (4)$$

The spin-dependent local density of states (LDOS) at a particular site i is given by the diagonal elements of the spectral density:

$$\rho_{i\sigma}(E) = \frac{1}{\hbar} A_{ii\sigma}(E - \mu) , \quad (5)$$

by which we can express, e.g., the spin- and site-dependent average occupation numbers

$$\langle n_{i\sigma} \rangle = \int_{-\infty}^{\infty} \frac{1}{e^{\beta(E-\mu)} + 1} \rho_{i\sigma}(E)\, dE \quad (6)$$

and the site-dependent charge density $\langle n_i \rangle = \langle n_{i\uparrow} \rangle + \langle n_{i\downarrow} \rangle$ and magnetization $m_i = \langle n_{i\uparrow} \rangle - \langle n_{i\downarrow} \rangle$ for each temperature T ($\beta = 1/k_B T$).

Since our study concerns ferro- as well as antiferromagnetism, we decompose the semi-infinite system of lattice sites into two chemically equivalent sublattices A and B. The decomposition is performed in such a way that *in the bulk* each sublattice fully reflects translational symmetry, i.e., the thermodynamical average of the occupation-number operator $\langle n_{i\sigma} \rangle$ shall be equal for all sites i belonging to the same sublattice. We do not exclude, however, a sublattice dependence. In the bulk we thus have

$$\langle n_{i\sigma} \rangle = \begin{cases} n_{A\sigma}, & i \in A \\ n_{B\sigma}, & i \in B . \end{cases} \quad (7)$$

The magnetic moments in each sublattice order, if at all, ferromagnetically

$$m_i = \begin{cases} m_A = n_{A\uparrow} - n_{A\downarrow}, & i \in A \\ m_B = n_{B\uparrow} - n_{B\downarrow}, & i \in B . \end{cases} \quad (8)$$

Spontaneous band magnetism is indicated by $m_A = m_B \neq 0$ for a ferromagnet and by $m_A = -m_B \neq 0$ for an antiferromagnet. For $m_A = m_B = 0$ we have a paramagnet. In all cases the spin- and site-independent band filling $\langle n \rangle$ is given by $\langle n_{i\uparrow} \rangle + \langle n_{i\downarrow} \rangle$.

When passing from the bulk to the surface, the situation becomes more complicated due to the breakdown of translational symmetry in the normal direction. We think the semi-infinite crystal to be built up from layers parallel to the surface. In the vicinity of the surface, an additional layer dependence of the average occupation numbers and thus of the magnetization has to be considered. Near the surface we therefore have $\langle n_{i\sigma} \rangle = n_{Al\sigma}$ ($\langle n_{i\sigma} \rangle = n_{Bl\sigma}$) and $m_i = m_{Al}$ ($m_i = m_{Bl}$) provided that the site i belongs to the sublattice A (B) and to the layer l. Within each layer l parallel to the surface perfect ferro- or antiferromagnetic ordering of the moments is assumed. The local density of states at sites near the surface will differ from bulk density of states only in the first few layers $l = 1, \ldots, L$ below the surface ($l = 1$ means the topmost surface layer). The same holds for the magneti-

zation: At the surface the size or even the direction of the magnetization may be quite different when compared with the bulk. With increasing l, however, the layer magnetization will soon approach the bulk value: $m_{Al=L+1}=m_A$, $m_{Bl=L+1}=m_B$. The number of surface layers L that at least have to be taken into account for convergence depends on the crystal structure, the type of the surface, and on details of the electronic structure; it must be determined by the actual calculation.

For certain conditions concerning the Coulomb interaction, the band filling and the temperature, there is more than one solution of the model as will be shown in the following. Apart from para- and ferromagnetic solutions, different kinds of antiferromagnetic solutions may be realized, since the decomposition of the lattice into sublattices is not unique. For zero temperature the internal energy $E_0=\langle H\rangle$ has to decide which solution is stable. E_0 can be expressed in terms of the spectral density:

$$E_0 = \frac{1}{2\hbar}\sum_{ij\sigma}\int_{-\infty}^{\infty}\frac{1}{e^{\beta E}+1}[T_{ij}+(E+\mu)\delta_{ij}]A_{ji\sigma}(E)\,dE\ . \tag{9}$$

For $T\neq 0$ the free energy F has to be considered:

$$F(T) = E_0(0)-T\int_0^T\frac{E_0(T')-E_0(0)}{T'^2}\,dT'\ . \tag{10}$$

The decisive quantity of our theory is the one-electron Green function (3). It is determined employing a mean-field (Hartree-Fock) approximation. In the equation of motion for $G_{ij\sigma}$,

$$(E+\mu)\,G_{ij\sigma}(E) = \hbar\,\delta_{ij} + \sum_k T_{ik}\,G_{kj\sigma}(E) + U\,\langle\langle c_{i\sigma}n_{i-\sigma};\,c_{j\sigma}^{\dagger}\rangle\rangle\ , \tag{11}$$

the higher-order Green function appearing on the right-hand side prevents us from a straightforward solution. In the mean-field approach it is replaced by

$$\langle\langle c_{i\sigma}n_{i-\sigma};\,c_{j\sigma}^{\dagger}\rangle\rangle \mapsto \langle n_{i-\sigma}\rangle\,G_{ij\sigma}(E)\ . \tag{12}$$

Now we are left with the following equation for the Green function:

$$(E+\mu-U\langle n_{i-\sigma}\rangle)\,G_{ij\sigma}(E) = \hbar\,\delta_{ij} + \sum_k T_{ik}\,G_{kj\sigma}(E)\ . \tag{13}$$

We notice that the equation of motion for $G_{ij\sigma}$ includes the average occupation number $\langle n_{i-\sigma}\rangle$, which in turn has to be determined via Eqs. (4), (5), and (6) from $G_{ij\sigma}$ itself. $\langle n_{i-\sigma}\rangle$ and $G_{ij\sigma}$ have thus to be calculated self-consistently. In the bulk the equation of motion is completely equivalent with the Stoner model. In this case we are allowed to exploit translational symmetry to solve Eq. (13). Restricting oneself to para- and ferromagnetism, the solution is easily obtained by Fourier transformation to the Bloch representation (see Ref. 11):

$$G_{ij\sigma}(E)=\frac{1}{N}\sum_{\mathbf{k}}e^{i\mathbf{k}(\mathbf{R}_i-\mathbf{R}_j)}\frac{\hbar}{E-[\epsilon(\mathbf{k})-\mu]-Un_{-\sigma}+i\,0^+}\ . \tag{14}$$

Here the occupation number $n_{-\sigma}=\langle n_{i-\sigma}\rangle$ is taken to be site independent. Considering additionally antiferromagnetism leads to complications, but still it is possible to derive an analytical expression for $G_{ij\sigma}$. Translational symmetry is now reflected by the sublattices, so transforming to the corresponding Bloch representation is appropriate (see Ref. 11). No analytical solution of Eq. (13) is possible, however, if the crystal surface is taken into account. So we have to look for a suitable technique allowing for a numerical evaluation of the theory.

III. RECURSION METHOD

A computationally feasible possibility to solve the equation of motion is provided by the recursion method. The main advantage of this method rests on its ability to deal with systems without translational symmetry. We will employ the recursion method to calculate the local density of states (LDOS) at the crystal surface. But also for calculating the bulk density of states the recursion scheme is rather useful, e.g., it avoids the $\mathbf{k}$ sum in Eq. (14). The method and its applications to the electronic structure of solids are outlined in Refs. 16 and 17. In the following we only briefly sketch the points that are essential for the present study.

Actually, the recursion method applies to a one-particle Hamiltonian and is commonly not used to deal with many-body interactions. Within the mean-field approximation, however, we can easily introduce an *effective* one-particle Hamiltonian that leads exactly to the same equation of motion (13) for the Green function (3):

$$H_{\rm eff} = \sum_{ij\sigma} h_{ij\sigma}^{\rm eff}\,c_{i\sigma}^{\dagger}c_{j\sigma}\ ,$$

$$h_{ij\sigma}^{\rm eff} = T_{ij}-\mu\,\delta_{ij}+U\,\langle n_{i-\sigma}\rangle\,\delta_{ij}\ . \tag{15}$$

We construct a unitary transformation so that $H_{\rm eff}$ becomes tridiagonal. Once the Hamiltonian is transformed into tridiagonal form, the diagonal elements of the Green function can be easily expressed as an infinite continued fraction:

$$G_{ii\sigma}(E)=G_{i\sigma}^{(0)}(E)\ ,$$

$$G_{i\sigma}^{(k)}(E)=\frac{\hbar}{E+i\,0^+-a_{i\sigma}^{(k)}-(b_{i\sigma}^{(k+1)})^2\,G_{i\sigma}^{(k+1)}(E)/\hbar}\ ,$$

$$k=0,1,2,\ldots\ , \tag{16}$$

from which we get the LDOS at the site i and for spin direction σ. The recursion coefficients $a_{i\sigma}^{(k)}$ and $b_{i\sigma}^{(k)}$ are the diagonal and the first off-diagonal elements of the transformed Hamiltonian, respectively. They can be calculated iteratively for each site i and spin direction σ. Let $|i\sigma\rangle=c_{i\sigma}^{\dagger}|\text{vac}\rangle$ be the Wannier state at site i and with spin index σ. Choosing $|0,i\sigma\rangle=|i\sigma\rangle$ for the starting orbital, the recursion coefficients are given by the following recurrence relations:

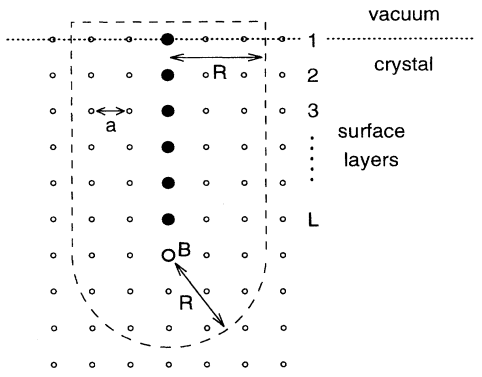

FIG. 1. Cluster of lattice sites used for the calculations. The cluster simulates the (100) surface of a simple cubic crystal with lattice constant a. L is the number of surface layers taken into account. Within each surface layer the central site is marked by a solid circle. For each marked site the distance from the cluster boundary is given by the radius R. Provided that R is sufficiently large, the cluster calculation yields the local density of states for the semi-infinite system at the marked central sites. The local density at site B corresponds to the bulk density of states. Typical values for R and L used: $R=10\,a$, $L=5$. Total number of sites: $N\approx 3800$.

$$a_{i\sigma}^{(0)}=\langle 0,i\sigma|\ H_{\text{eff}}\ |0,i\sigma\rangle,$$

$$b_{i\sigma}^{(1)}=||(H_{\text{eff}}-a_{i\sigma}^{(0)})|0,i\sigma\rangle||,$$

$$|1,i\sigma\rangle=\frac{1}{b_{i\sigma}^{(1)}}(H_{\text{eff}}-a_{i\sigma}^{(0)})|0,i\sigma\rangle\ , \tag{17}$$

and for $k\geq 1$:

$$a_{i\sigma}^{(k)}=\langle k,i\sigma|\ H_{\text{eff}}\ |k,i\sigma\rangle,$$

$$b_{i\sigma}^{(k+1)}=||(H_{\text{eff}}-a_{i\sigma}^{(k)})|k,i\sigma\rangle-b_{i\sigma}^{(k)}|k-1,i\sigma\rangle||,$$

$$|k+1,i\sigma\rangle=\frac{1}{b_{i\sigma}^{(k+1)}}[(H_{\text{eff}}-a_{i\sigma}^{(k)})|k,i\sigma\rangle-b_{i\sigma}^{(k)}|k-1,i\sigma\rangle]\ . \tag{18}$$

For the calculation of the internal energy by Eq. (9) we also need off-diagonal elements of the Green function $G_{ij\sigma}$. They are derived from a polarization relation:

$$G_{ij\sigma}(E)=\langle\langle c_{i\sigma};\ c_{j\sigma}^{\dagger}\rangle\rangle_E=\tfrac{1}{4}(\langle\langle c_{i\sigma}+c_{j\sigma};\ c_{i\sigma}^{\dagger}+c_{j\sigma}^{\dagger}\rangle\rangle_E - \langle\langle c_{i\sigma}-c_{j\sigma};\ c_{i\sigma}^{\dagger}-c_{j\sigma}^{\dagger}\rangle\rangle_E)\ . \tag{19}$$

To get the Green functions on the right-hand side, appropriate starting orbitals for the recurrence relations, $|0,i+j\ \sigma\rangle=(|i\sigma\rangle+|j\sigma\rangle)/\sqrt{2}$ and $|0,i-j\ \sigma\rangle=(|i\sigma\rangle-|j\sigma\rangle)/\sqrt{2}$, respectively, have to be chosen.

IV. COMPUTATIONAL DETAILS

For the numerical evaluation of the theory it is necessary to consider a cluster that consists of a finite number of sites instead of the semi-infinite lattice. This ensures a finite dimension D of the Hilbert space and thus of the vectors and matrices in Eqs. (17) and (18). Due to spin degeneracy, D is given by twice the number of sites N. Since the Hamiltonian (15) does not couple states of opposite spin direction, the calculation of the LDOS at a site i can be done separately for each spin direction σ. So N-dimensional vectors and matrices are necessary for applying the recursion scheme. The cluster of sites used for the calculations is shown schematically in Fig. 1. As we have assumed perfect translational symmetry within each layer parallel to the surface, it is sufficient to take into account the LDOS at one particular site inside each layer. The cluster LDOS resembles the LDOS of the semi-infinite system best at those sites in the cluster that have maximum distances to the cluster boundary.

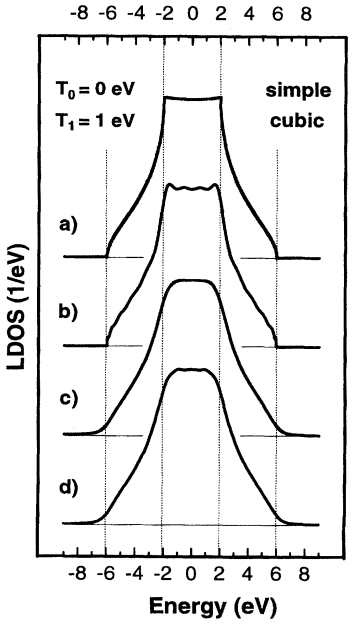

FIG. 2. Bulk local density of states for a simple cubic crystal. T_0 and T_1 denote the on-site and the nearest-neighbor hopping integral, respectively. (a) Exact bulk LDOS from Ref. 18. (b) Recursion method with quadratic termination ($R=10\,a$, $K=14$, see text). (c) Exact LDOS, but convoluted with a Lorentzian ($\Gamma=W/100$) and with a Gaussian profile ($\alpha=W/20$), see text. (d) Recursion method with constant termination ($R=10\,a$, $K=50$) and using Lorentz and Gauss convolution ($\Gamma=W/100$, $\alpha=W/20$), see text.

The recursion method is most efficient in the case of a tight-binding Hamiltonian. For reasons of computational feasibility we therefore consider on-site and nearest-neighbor hopping only. The corresponding hopping integrals are denoted by T_0 and T_1, respectively. T_0 defines the energy zero. The nearest-neighbor hopping integral is fixed at $T_1=1.0$ eV. T_1 determines the width W of the bulk LDOS. For the simple cubic crystal considered here, we have $W=2\,z_1^{(B)}T_1=12$ eV. Figure 2 shows the bulk local density of states. We compare the exact density of states from Ref. 18 [Fig. 2(a)] with the results of the recursion method. We have applied two different techniques concerning the termination of the infinite continued-fraction representation of the Green function (16).

First, we used a quadratic termination of the continued

fraction. Thereby we have assumed the recursion coefficients to be convergent for $k \mapsto \infty$: $a_{i\sigma}^{(k)} \mapsto a_{i\sigma}$ and $b_{i\sigma}^{(k)} \mapsto b_{i\sigma}$ (cf. Ref. 19). We thus may replace $G_{i\sigma}^{(k)}$ by the remainder $G_{i\sigma}^{(\infty)}$ at some level $k=K$:

$$G_{i\sigma}^{(\infty)}(E) = \frac{1}{2(b_{i\sigma})^2}[E-a_{i\sigma} \pm \sqrt{(E-a_{i\sigma})^2-4(b_{i\sigma})^2}\ ] . \tag{20}$$

We have to ensure that K is as large so that the Kth recursion coefficients do not differ too much from their asymptotic limits. Furthermore, a sufficiently large cluster has to be chosen in order to avoid strong disturbing effects induced by the cluster boundary (see Refs. 16 and 17). With the quadratic termination the exact LDOS is approximated rather well [Fig. 2(b)]. Especially, the band edges are reproduced exactly, some discrepancies, however, remain in the vicinity of the van Hove singularities at $E=\pm 2$ eV.

A quadratic termination of the continued fraction will fail to yield reasonable results if the recursion coefficients do not converge. It is well known that the coefficients exhibit oscillatory behavior if the LDOS shows a gap.[19] This prevents us from using the quadratic termination particularly in the case of an antiferromagnet, since for strong Coulomb interaction U the Slater gap manifests itself in the LDOS.[11] To be consistent the method of quadratic termination is therefore avoided in all cases here, i.e., for the para- and the ferromagnet, too.

Instead, we will consider another possibility. Since the states $|k,i\sigma\rangle$ form an orthonormal set, the continued fraction must terminate at some level $K \leq N$ (i.e., $b_{i\sigma}^{(K+1)}=0$). The resulting LDOS is the exact cluster LDOS (at site i) and thus consists of a finite number of weighted δ peaks at different energies. To approximate the LDOS of the semi-infinite system, we therefore convolute the cluster LDOS with a Lorentzian and a Gaussian profile. Lorentz convolution is performed by replacing the infinitesimal $i\,0^+$ in Eq. (16) by $i\,\Gamma$, where Γ is a small positive number. This implies a broadening of the δ peaks and so allows for using a discrete energy mesh in the numerical calculation. After that the LDOS is smeared out by convolution with a Gaussian profile $\sim\exp(E^2/\alpha^2)$. It turns out that due to the convolution procedure it is not necessary to include all recursion coefficients until termination of the continued fraction. Actually, a rather small number (typically $K=50$) is sufficient. Taking into account more coefficients does not affect the shape of the LDOS at all.

Figure 2(c) shows the exact bulk LDOS [see 2(a)] but Lorentz and Gauss convoluted with $\Gamma=W/100$ and $\alpha=W/20$, respectively. These are the maximum values used for the following calculations. Comparing with the result of the recursion method in Fig. 2(d) ($K=50$, $\Gamma=W/100$, and $\alpha=W/20$), proves that the recursion scheme almost perfectly yields the exact but smoothed LDOS. The method is easy to handle and reliable in the whole parameter range of U, $\langle n\rangle$, and T. Ferromagnetic as well as antiferromagnetic configurations can be treated, and no difficulties appear when the crystal surface is taken into account. Moreover, systematic improvement is possible, simply by enlarging the cluster that underlies the calculation. We like to point out that smoothing the LDOS has only minor effects on integral quantities such as the magnetization or the free energy, which are of particular interest for our study.

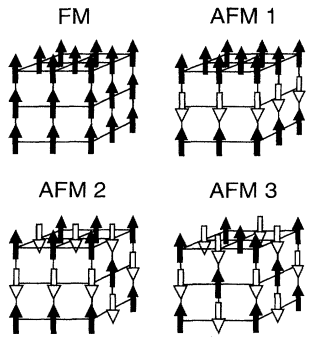

FIG. 3. Different magnetic structures for a simple cubic crystal. FM denotes the ferromagnetic structure. Depending on the decomposition of the lattice into the sublattices, different antiferromagnetic structures can be realized. The structures AFM1, AFM2, and AFM3 have been considered in the calculations.

Our calculations for investigating effects of surface magnetism are performed as follows. Before solving the model for the crystal surface we have to consider the bulk. For a given set of U, $\langle n\rangle$, and T, Eqs. (3)–(6) and Eq. (13) are solved self-consistently making use of translational symmetry by Eq. (7). We determine the spin-dependent average occupation numbers and the chemical potential. These quantities can be held constant in the subsequent calculation that includes the crystal surface, and only the spin- and layer-dependent average occupation numbers for the surface layers have to be calculated. Thus, if L surface layers are taken into account, there are $2L$ parameters to be determined self-consistently.[20] We include as many surface layers in the calculation as necessary to ensure that the layer-dependent average occupation numbers approach their bulk values smoothly.

V. RESULTS AND DISCUSSION

A. Bulk phase diagram

The effort to investigate surface magnetism must start with the bulk material. With respect to bulk magnetic properties our mean-field approach is equivalent to the Stoner model of magnetism. In the following we focus on those aspects of the Stoner model necessary for the subsequent discussion of surface magnetism.

Apart from paramagnetic and ferromagnetic (FM) solutions we make allowances for various kinds of antiferromagnetic (AFM) solutions, which are given by certain decompositions of the simple cubic lattice into the sublattices. Figure 3 shows the different magnetic structures considered. The ferromagnetic structure FM and the three antiferromagnetic AFM1, AFM2, and AFM3 shown in Fig. 3 are the magnetic structures of highest symmetry. The magnetic moments order ferromagnetically within the (100) planes for the AFM1 structure, within the (110) planes for the AFM2 structure, and finally, for the AFM3 structure, within the (111) planes. For a magnetic moment m_i at a particular site i, the number of nearest-neighbor sites with magnetic moments

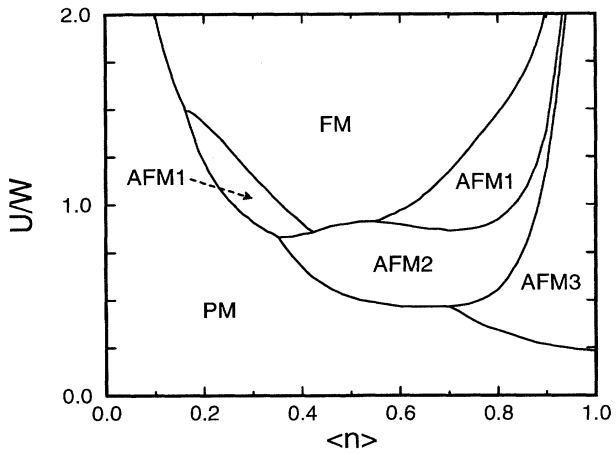

FIG. 4. Bulk magnetic phase diagram for $T=0$ in terms of the band filling $\langle n\rangle$ and the ratio between Coulomb interaction U and the width of the free Bloch band W. The lines represent the boundaries between the paramagnetic (PM), the ferromagnetic (FM), and the different antiferromagnetic phases (AFM1, AFM2, AFM3). The phase diagram is symmetric to the $\langle n\rangle=1$ axis. The region between $\langle n\rangle=1$ and $\langle n\rangle=2$ is therefore attainable by reflection at the $\langle n\rangle=1$ axis.

coupled ferromagnetically to m_i decreases from $z_1^{(3)}=6$ for the FM structure to $z_1^{(2)}=4$ for the AFM1, $z_1^{(1)}=2$ for the AFM2, and to $z_1^{(0)}=0$ for the AFM3 structure. $z_1^{(n)}$ is also the number of nearest neighbors in the simple n-dimensional lattice.

In the following we discuss some results obtained for zero temperature. Figure 4 shows the magnetic phase diagram in terms of the band filling $\langle n\rangle$ and the ratio between the Coulomb interaction and the width of the free Bloch band U/W. We found a nonmagnetic (paramagnetic) solution to exist for each U and each $\langle n\rangle$. Under certain conditions, however, magnetic solutions may appear additionally. Indeed, in wide regions of the $(U,\langle n\rangle)$ plane all the magnetic solutions that have been considered are existing. Thus we have systematically calculated the internal energy of each solution in the entire parameter plane. The phase diagram indicates which of the solutions is most stable for a certain parameter constellation.

If there is more than one solution, it is always the paramagnetic one that is most unstable. Generally, the system tends to be paramagnetic only for small band occupations $\langle n\rangle$ and not too high Coulomb interaction U. For each $\langle n\rangle$ there is a critical $U(\langle n\rangle)$, above which the system becomes ferromagnetic. For not too small band filling the ferromagnetic region is separated from the paramagnetic one by at least one antiferromagnetic phase. Antiferromagnetism dominates around the $\langle n\rangle=1$ axis, but even down to $\langle n\rangle=0.17$, the AFM1 phase is found to be stable in a small interval of U values. We notice that there are two AFM1 regions that are not connected but separated by the AFM2 phase, which turns out to be stable against the AFM1 phase near $\langle n\rangle=0.5$.

Let us now focus attention on the case of the exactly half-filled valence band, i.e., $\langle n\rangle=1$. No magnetic solutions are found for sufficiently weak Coulomb interaction U.[21] For all U exceeding the critical value $U_c^{\mathrm{AFM3}}=0.23\ W$ antiferromagnetic solutions of AFM3 type are found to be existing. We find antiferromagnetic solutions AFM2 for $U>U_c^{\mathrm{AFM2}}=0.47\ W$, and solutions AFM1 above $U_c^{\mathrm{AFM1}}=0.48\ W$. Finally, ferromagnetism becomes possible at $U_c^{\mathrm{FM}}=0.58\ W$. Thus increasing U implies a certain sequence of the different magnetic structures on the $\langle n\rangle=1$ axis. The same sequence is observed when approaching the $\langle n\rangle=1$ axis for a sufficiently strong Coulomb interaction U as can be seen from Fig. 4. Moreover, this corresponds to the energetic order of the solutions on the $\langle n\rangle=1$ axis. Magnetic solutions of all types exist for $U>U_c^{\mathrm{FM}}$, the AFM3 solution always being the most stable one, followed by antiferromagnetic solutions of the AFM2 and then of the AFM1 type. Finally, ferromagnetism is most unstable.

To understand the energetic order of the magnetic solutions for $\langle n\rangle=1$ and strong Coulomb interaction U, we consider a partitioning of the Hubbard Hamiltonian into on-site terms (on-site hopping and Coulomb interaction) and nearest-neighbor hopping terms. It is well known that within perturbation theory of the second order in $T_{i\neq j}$ the Hubbard model at half filling can be transformed into an effective Heisenberg model with exchange integrals given by $J_{ij}\sim -T_{ij}^2/U$.[22] Thus an electron hopping from site i to one of the nearest-neighbor sites j and back to i again *gains* energy. Due to the Pauli principle, however, at half filling such (virtual) processes are only possible if the spins of electrons at the sites i and j are opposite. From this we may conclude that compared with antiferromagnetism ferromagnetism is not stable, which has been found indeed. Turning to the different antiferromagnetic phases, we argue that the ground-state energy is determined by the number of nearest neighbors with magnetic moments opposite to the magnetic moment at a given arbitrary site i. In the AFM3 phase each site i has the maximum number of $z_1^{(3)}-z_1^{(0)}=6$ nearest neighbors belonging to the other sublattice. This explains why the AFM3 structure is the most stable one, followed by the AFM2 structure $(z_1^{(3)}-z_1^{(1)}=4)$ and the AFM1 structure $(z_1^{(3)}-z_1^{(2)}=2)$.

Concludingly, as the $T=0$ phase diagram (Fig. 4) is concerned, the Stoner model leads to physically quite plausible results. Despite the simplicity of the mean-field approach, the general trends seem to be correct. It should be mentioned, however, that the mean-field approximation generally overestimates the possibility for spontaneous magnetization, which is rather obvious when compared to more sophisticated many-body approaches. Different theories[11,15,23] predict a minimum band occupation below which magnetic order is impossible. In the Stoner model, on the other hand, such a critical band filling does not appear. Here, however, we like to point out once more that it is not the aim of our study to give a highly accurate description of band magnetism but to provide a starting point for the investigation of surface magnetism. If the general trends are correct, the mean-field approximation should be suited for a first insight into magnetic effects that are due to the presence of the crystal surface.

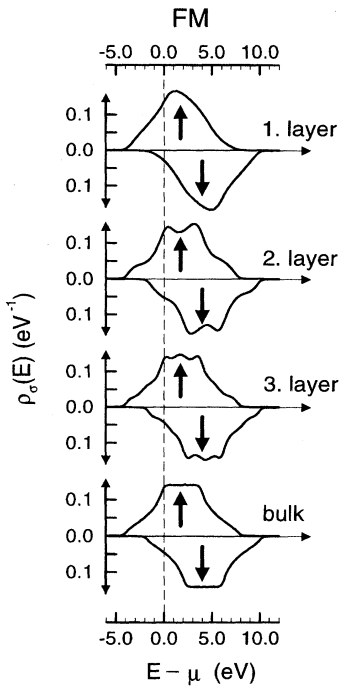

FIG. 5. Spin- and layer-dependent local density of states ρ (LDOS) as function of energy E for a self-consistent ferromagnetic solution (FM) at zero temperature. Coulomb interaction $U=12.6$ eV$=1.05$ W. Band filling $\langle n\rangle=0.3$. Layer magnetizations: $m=0.234$ (first), $m=0.165$ (second), $m=0.180$ (third), $m=0.180$ (bulk). Parameters of calculation (see text and Figs. 1 and 2 for key to symbols): $R=17$ a, $L=9$, $K=60$, $\Gamma=W/200$, and $\alpha=W/40$.

B. Local density of states

Our main interest is focused on electronic and magnetic properties in the vicinity of the surface, which has been chosen to be the (100) surface of a simple cubic crystal for the present study. Due to the reduced coordination number of atoms within the topmost surface layer, electrons tend to be more localized at the surface when compared with the bulk. It is expected that this can have considerable consequences for spontaneous magnetic order at the surface. All such effects will manifest themselves in the local density of states (LDOS) at sites near the surface, which is a key quantity as far as electronic and magnetic properties are concerned.

Figure 5 shows the LDOS at sites within the topmost surface layer as well as within the second and the third layer below the surface in comparison with the LDOS in the bulk. The Coulomb interaction and the band filling have been fixed at $U=12.6$ eV$=1.05$ W ($W=12$ eV) and $\langle n\rangle=0.3$, respectively. The LDOS shown in Fig. 5 corresponds to a self-consistent ferromagnetic solution (FM) of the equation of motion (13) at zero temperature. Therefore, the LDOS in the bulk but also in each surface layer exhibits an exchange splitting, which results in a nonzero layer-dependent magnetization.

The bulk LDOS reflects the well-known Stoner picture for band ferromagnetism. Due to the Coulomb interaction U the free Bloch band splits up into two spin-dependent subbands, which are nondeformed but shifted rigidly against one another by $U\cdot m$. Here the bulk magnetization amounts to $m=0.180$.

Compared with the bulk LDOS, the LDOS in the surface layers is considerably distorted. The deviations are the more pronounced the nearer the layer is located to the surface. The shape of the LDOS in the topmost surface layer exhibits the most significant changes with respect to the bulk. In the calculation up to nine surface layers have been included, the spin-dependent average occupation numbers of which have all been determined independently. It turns out that already the LDOS in the fifth layer below the surface is hardly to be distinguished from the bulk LDOS. Integral quantities, such as the average occupation numbers, converge even faster to their bulk values with increasing distance from the surface. So for the third layer and all subsequent ones the occupation numbers are constant within numerical accuracy.

For a more detailed discussion, introduction of the moments of the LDOS at a site i and for spin index σ may be helpful:

$$M_{i\sigma}^{(n)} = \int_{-\infty}^{\infty} E^n \, \rho_{i\sigma}(E+\mu)\, dE \, . \tag{21}$$

Alternatively, we can write [cf. Eq. (15)]:

$$M_{i\sigma}^{(n)} = \sum_{i_1 \cdots i_{n-1}} h_{ii_1\sigma}^{\mathrm{eff}} h_{i_1 i_2 \sigma}^{\mathrm{eff}} \cdots h_{i_{n-1} i\sigma}^{\mathrm{eff}} . \tag{22}$$

For a ferro- or for a paramagnet the average occupation number in the bulk is site independent because of translational symmetry: $\langle n_{i\sigma}\rangle=\langle n_\sigma\rangle$. If, for the moment being, we choose the energy zero to coincide with $h_{ii\sigma}^{\mathrm{eff}}=h_\sigma^{\mathrm{eff}}=T_0-\mu+U\langle n_{-\sigma}\rangle$ for a fixed spin direction σ under consideration, all terms in Eq. (22) will vanish exept for terms that excludingly consist of nearest-neighbor elements $h_{i\neq j\sigma}^{\mathrm{eff}}$. Since there is no way to start from and to return to a given site i by an *odd* number of nearest-neighbor hoppings for a simple cubic lattice, all odd moments $M_{i\sigma}^{(2n+1)}$ vanish. Therefore, the bulk LDOS $\rho_\sigma(E)$ is a symmetric function of energy with respect to its center of gravity $T_0-\mu+U\langle n_{-\sigma}\rangle$. For the layers near the surface, however, the occupation numbers $\langle n_{i\sigma}\rangle$ and thus the elements $h_{ii\sigma}^{\mathrm{eff}}$ are no longer independent of i, which results in nonzero odd moments. So the symmetry of the LDOS at sites in the vicinity of the surface is distorted. Generally, the deviations from mirror symmetry are strongest at the very surface becoming smaller and smaller when passing to the bulk (see Fig. 5). This is quite different to the case of the "free" system: For $U=0$ the LDOS in each layer must be a symmetric function of energy.[24]

In contrast to the bulk situation, the LDOS at sites near the surface does not show a *rigid* exchange splitting, as can be seen most clearly looking at the spin-dependent LDOS for the first and the second layer in Fig. 5. However, for each layer there seems to remain a symmetry between the LDOS for $\sigma=\uparrow$ and $\sigma=\downarrow$. Indeed, the equation of motion (13) for $\sigma=\downarrow$ becomes formally identical with the equation of motion for $\sigma=\uparrow$ if we consider the following substitutions:

$$E \mapsto -E+2(T_0-\mu)+U\langle n_i\rangle \ ,$$

$$T_{i\neq j} \mapsto -T_{i\neq j} ,$$

$$G_{ij\downarrow} \mapsto -G_{ij\downarrow} . \tag{23}$$

Here $\langle n_i\rangle$ is the charge density at the site i: $\langle n_i\rangle=\langle n_{i\uparrow}\rangle+\langle n_{i\downarrow}\rangle$. The LDOS at each site is not affected by the second substitution at all, since, similar to the argument given above, the LDOS will only depend on even powers of $T_{i\neq j}$ for a (semi-infinite) simple cubic lattice. Provided that we are allowed to assume layerwise charge neutrality, $\langle n_i\rangle=\langle n\rangle$, we may derive the following symmetry relation from (23):

$$\rho_{i\uparrow}(E) = \rho_{i\downarrow}(-E+2T_0+U\langle n\rangle) . \tag{24}$$

The calculated LDOS for the layers shown in Fig. 5 satisfies the symmetry relation very well but not exactly. This is due to a charge transfer from the first and from the second layer to the bulk: We have $\langle n_i\rangle-\langle n\rangle=-0.002$, -0.003, and 0.000 for the first, the second, and the third layer below the surface, respectively. This small charge transfer is necessary to ensure a common Fermi level of all surface layers and the bulk in the self-consistent calculation.

Contrary to the small charge transfer there is a considerable change of the surface-layer magnetizations with respect to the bulk magnetization. The magnetization of the topmost surface layer amounts to $m=0.234$, which means an increase by 30% with respect to the bulk magnetization $m=0.180$. In the second layer the magnetization turns out to be smaller than the bulk magnetization ($m=0.165$), while for the third and all subsequent layers the magnetization is equal to the bulk magnetization within numerical uncertainty. The enlarged magnetization of the topmost layer (and the reduced magnetization of the second layer) is not due to an additional Stoner-like shift of the spin-dependent subbands. For a given spin direction σ the band edges of the LDOS for each surface layer coincide with the band edges of the bulk LDOS. The layer by layer variations in the effective atomic energy level $h_{ii\sigma}^{\text{eff}}=T_0-\mu+U\langle n_{i-\sigma}\rangle$ are not that much pronounced to produce states outside the bulk band. Therefore, the change of magnetization near the surface is a density-of-states effect. Compared with the bulk LDOS, the LDOS of the first layer is much more compressed ("band narrowing"). This can easily be verified considering the second moment of the LDOS:

$$\Delta^2\rho \equiv M_{i\sigma}^{(2)}-(M_{i\sigma}^{(1)})^2 = \sum_{j\neq i} (T_{ij})^2 = z_1(i)\ T_1^2 , \tag{25}$$

where $z_1(i)$ denotes the number of nearest neighbors for a site i. So $\Delta\rho$ is reduced with respect to the bulk value because of the lower coordination number of atoms within the topmost surface layer. For the second and the third surface layer higher moments have to be considered.

Figure 6 shows the surface-layer and bulk LDOS corresponding to an antiferromagnetic solution of AFM1 type. We have assumed the magnetic moments to order ferromagnetically within the (100) layers parallel to the surface. The magnetization changes its direction when passing from layer to layer. Again we fixed the band filling at $\langle n\rangle=0.3$. The Coulomb interaction is $U=11.4$ eV$=0.95\ W$.

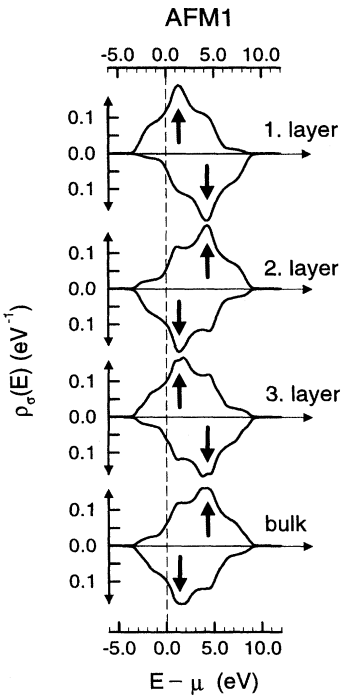

FIG. 6. Spin- and layer-dependent local density of states ρ (LDOS) as function of energy E for a self-consistent antiferromagnetic solution (AFM1) at zero temperature. Layers parallel to the (100) surface order ferromagnetically. Coulomb interaction $U=11.4$ eV$=0.95\ W$. Band filling $\langle n\rangle=0.3$. Layer magnetizations (absolute values): $m=0.188$ (first), $m=0.116$ (second), $m=0.110$ (third), $m=0.101$ (bulk). Parameters of calculation: see Fig. 5.

Let us first discuss the bulk LDOS which is shown in Fig. 6 for a certain lattice site belonging to one of the two sublattices A or B. The LDOS at a site belonging to the other sublattice is simply generated by exchanging the $\uparrow$ subband with the $\downarrow$ subband. Contrary to the ferromagnet, the bulk LDOS for $\sigma=\uparrow$ occupies exactly the same energy range as the LDOS for $\sigma=\downarrow$ at the same site (see Fig. 6). However, the centers of gravity of the $\uparrow$ and the $\downarrow$ subband are shifted against one another by $U\cdot|m|$. For the example shown, the Coulomb interaction is not strong enough to open a gap in the LDOS although the Slater gap is present at each $\mathbf{k}$ point of the first Brillouin zone. The bandwidth is still given by the width of the free Bloch band $W=12$ eV. The bulk sublattice magnetization amounts to $|m|=0.101$.

Qualitatively, the LDOS at sites near the surface is similar to the bulk LDOS. In particular, the LDOS of all surface layers and for both sublattices in the bulk share common band edges. As for the ferromagnetic case discussed before, the layer by layer variations of the average occupation numbers $\langle n_{i\sigma}\rangle$ are considerable but not strong enough to result in split-off states. The shape of the LDOS near the surface, however, clearly deviates from the shape of the bulk LDOS, and the change is most pronounced for the topmost surface layer. But already for the fifth layer the LDOS can hardly be distinguished from the bulk LDOS as in the ferromagnetic

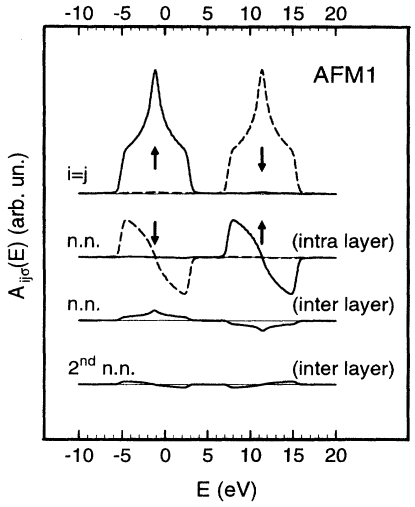

FIG. 7. Bulk spectral density $A_{ij\sigma}$ as function of energy for an antiferromagnet of the AFM1 type [ferromagnetic order within (100) planes, magnetization alternating layer by layer]. Calculation at zero temperature for $U=1.5\ W$ and $\langle n\rangle=0.7$. On-site spectral density, $i=j$ (first from top). Off-diagonal element of the spectral density for nearest-neighbor (n. n.) sites i and j belonging to the same sublattice, i.e., the same (100) layer (second from top). i and j nearest neighbors, but belonging to different sublattices, i.e., neighboring layers (third). i and j belonging to different sublattices as before but being second-nearest neighbors (fourth). For the last two cases ↑ and ↓ spectral densities are identical.

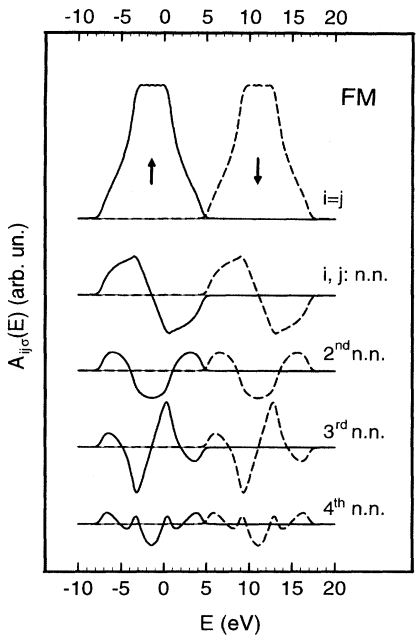

FIG. 8. Bulk spectral density $A_{ij\sigma}$ as function of energy for the ferromagnet. Calculation at zero temperature for $U=1.5\ W$ and $\langle n\rangle=0.7$. On-site ($i=j$) and off-diagonal spectral density, where the sites i and j are nearest neighbors, second-nearest neighbors, etc.

case. Again, the charge-transfer effects are small. We found $\langle n_i\rangle-\langle n\rangle=-0.004$, 0.001, and 0.001 for the first, the second, and the third layer below the surface, respectively. On the other hand, there are drastic effects with respect to the layer magnetization. Compared with the bulk value, the topmost layer magnetization is increased by about 86% and amounts to $|m|=0.188$. An enhanced magnetization is observed for the second ($|m|=0.116$) and for the third layer ($|m|=0.110$) as well.

In Fig. 7 the bulk spectral density for the case of an AFM1 type antiferromagnet is shown. We now consider a stronger Coulomb interaction ($U=1.5\ W$) and a higher band filling ($\langle n\rangle=0.7$). The on-site spectral density for $i=j$ is directly related to the LDOS at the site i. For the parameters considered now, the Slater gap is also visible in the LDOS: Both, the ↑ and the ↓ band, split into two subbands, the one of which, however, has very small spectral weight. Corresponding ↑ and ↓ subbands occupy exactly the same energy range. This prevents the sublattice magnetization ($|m|=0.678$) from being saturated even at $T=0$.

Furthermore, Fig. 7 shows some off-diagonal elements of the spectral density $A_{ij\sigma}$. These are of special interest, since they are related to the probability for an additional electron to move from a site i to a site j in the lattice. As can be read off from Fig. 7, intrasublattice propagation dominates against intersublattice propagation, i.e., electrons preferably move *within* the ferromagnetically ordered (100) planes, while motion between two neighboring layers is almost negligible. If we forget about the subbands with small spectral weights for a moment, the ↑ and the ↓ LDOS at a particular site i of the sublattice A are energetically well separated from each other. The LDOS at a site j belonging to sublattice B is obtained by interchanging the ↑ with the ↓ LDOS at site i. Therefore, the ↑ LDOS at site i and the ↑ LDOS at site j are energetically well separated, too, and an ↑ electron's wave function that is located within a layer belonging to a certain sublattice will rapidly decay outside the layer: There are no (only few) states of the same energy the wave function can couple to. So, provided that the Slater gap shows up in the LDOS, propagation of electrons is more or less confined to two dimensions. The two-dimensional character also manifests itself in the shape of the LDOS: Apart from the subband with small spectral weight, the line shape for each spin direction is nearly the same as the shape of the free Bloch density of states for a simple *square* lattice. The bandwidth is equal to $2z_1^{(2)}T_1=8$ eV, where $z_1^{(2)}=4$ is the number of nearest neighbors for the square lattice.

For the other types of antiferromagnetic order (see Fig. 3) the situation is similar: If there is a Slater gap visible in the LDOS, the propagation of electrons is restricted to mere intrasublattice propagation. The effect is the more pronounced the wider the gap. For the AFM2 phase the resulting LDOS is quasi-one dimensional, and for the AFM3 phase zero dimensional, i.e., for each spin direction the LDOS reduces to a δ peak. In this case a finite width of the LDOS could only be expected, if the Hamiltonian included terms allowing for hopping between second-nearest neighbors.

These results for the antiferromagnetic phases may be compared with the corresponding results for the ferromagnet shown in Fig. 8. For the same Coulomb interaction and the same band filling the ↑ and ↓ LDOS are energetically just

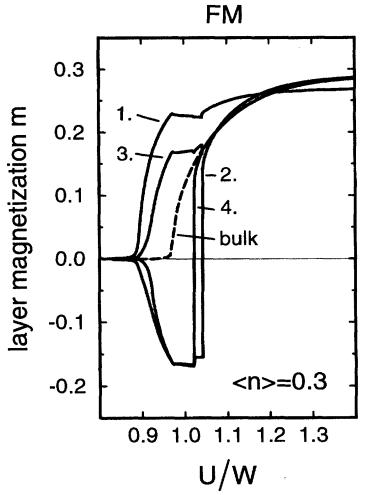

FIG. 9. Magnetizations of the first four layers below the surface (solid lines, calculation for the semi-infinite system) and bulk magnetization (dashed line, calcuation for the infinite system without surface). Magnetizations given as functions of the ratio between Coulomb-interaction and Bloch-band width U/W for $\langle n\rangle = 0.3$ at zero temperature. Further parameters: $L = 12$, $R = 10\,a$, $\Gamma = W/100$, and $\alpha = W/20$.

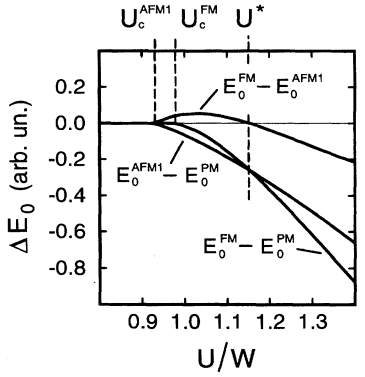

FIG. 10. Differences ΔE_0 between the internal energies of the paramagnetic (PM), the ferromagnetic (FM), and an antiferromagnetic solution (AFM1) as functions of U/W ($\langle n\rangle = 0.3$, $T = 0$). U_c^{FM} and U_c^{AFM1} denote the critical Coulomb-interaction strengths for the existence of FM and AFM1 solutions. U^* marks the first-order phase transition.

separated from each other, the magnetization is saturated: $m = 0.700$ (fully polarized state, $\langle n_\downarrow\rangle = 0$). The off-diagonal elements of the spectral density $A_{ij\sigma}$ are non-negligible even for fourth-nearest-neighbor sites i and j. Generally, however, the absolute values of the spectral density are observed to become smaller and smaller with increasing distance between the sites i and j.

C. Layer magnetization

In the following we investigate the dependence of the magnetization on the model parameters U and $\langle n\rangle$ for layers near the surface and compare with the results for the bulk magnetization. The main task is to show up the general trends and to look for qualitative new effects.

Figure 9 shows the magnetization of the first four surface layers for $\langle n\rangle = 0.3$ and $T = 0$ as functions of the Coulomb interaction U. These result from a calculation for the semi-infinite system, where $L = 12$ surface layers have been taken into account (solid lines). Additionally, Fig. 9 shows the bulk magnetization that results from a calculation considering the three-dimensional, infinite lattice without surface (dashed line). In the range $U/W = 0.92 - 1.04$ the calculation that includes the surface yields an (AFM1) antiferromagnetic ordering of the magnetic moments in the bulk: The bulk sublattice magnetizations are almost identical with the magnetization of the third and the fourth layer, respectively; a clearly different magnetization is found for the first and for the second layer only. Within the considered range for U no ferromagnetic solution can be found when performing the calculation for the semi-infinite system. This is in remarkable contrast to the bulk calculation: In this case a ferromagnetic solution exists for all U above $U_c^{FM} = 0.97\ W$.

For the interpretation of this finding let us focus on Fig. 10 for a moment, where the internal energies of the FM and of the AFM1 magnetic solutions and of the paramagnetic solution (PM) are compared with each other (see also the phase diagram, Fig. 4). Again the calculations have been performed for the infinite system without surface. For strong Coulomb interaction U the FM solution is stable against the AFM1 solution. At $U = U^* = 1.15\ W$ there is a first-order transition from the ferromagnetic to the antiferromagnetic phase. This becomes obvious when following the line of minimal internal energy which exhibits a noncontinuous derivative at $U = U^*$. Finally, the system undergoes a second-order phase transition to the paramagnetic state at $U = U_c^{AFM1} = 0.92\ W$. However, if the Coulomb interaction is decreased "slowly" from $U > U^*$ to $U < U^*$, the system will remain in the ferromagnetic state even for $U < U^*$ until there is a second-order phase transition at $U = U_c^{FM}$, where the system becomes paramagnetic.

For $U < U^*$, however, the ferromagnetic state is instable with respect to small perturbations of the ideal, infinitely periodic lattice. This manifests itself in the semi-infinite system, where the crystal surface represents an immanent perturbation. Indeed, the drastic change of the layer magnetizations below $U = 1.04\ W$ (Fig. 9) indicates the point at which this perturbation is strong enough to destroy the metastable ferromagnetic order. In detail, we observe that the semi-infinite system first remains in the (metastable) ferromagnetic state. Then at $U = 1.04\ W$ the magnetization of the second layer immediately switches its sign. This leads to a small but clearly visible response in the magnetizations of the neighboring first and third surface layer. At a slightly lower value of U it is the fourth layer, the magnetization of which becomes inverted. Again, in response, a small noncontinuous change in the magnetization is observed for the second and the third layer. Within numerical accuracy the magnetizations of the fourth, the sixth, and all other even-numbered layers switch from $\uparrow$ to $\downarrow$ at the same value for U. If there is a

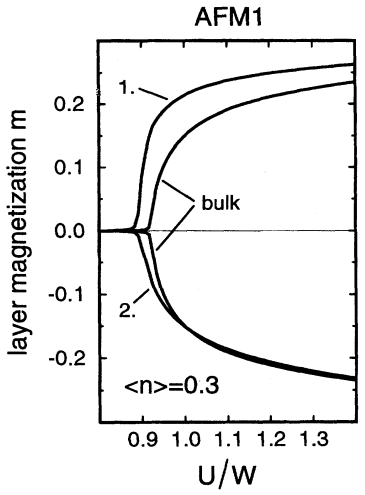

FIG. 11. Magnetizations of the first and the second surface layer and bulk sublattice magnetizations as functions of U/W ($\langle n\rangle = 0.3$, $T=0$) for the AFM1-type antiferromagnet [the moments within layers parallel to the (100) surface order ferromagnetically]. Parameters: $L=5$, $R=10\,a$, $\Gamma = W/100$, and $\alpha = W/20$.

further decrease in U, the layer magnetizations nearly remain constant until at $U \approx 0.97W$ the layer magnetizations coincide with the corresponding layer magnetizations of the AFM1 solution. We conclude that the crystal surface as an immanent perturbation of the periodic lattice is responsible for the actual transition from the metastable ferromagnetic to the stable antiferromagnetic state. The transition is not immediate, but starts from the very surface and then quickly penetrates into the bulk layer by layer.

In contrast to ferromagnetic solutions, antiferromagnetic solutions (AFM1) are found to be existing for every value of the Coulomb interaction $U > U_c^{\mathrm{AFM1}}$. The presence of the surface in the semi-infinite system does not exclude metastable antiferromagnetic solutions for $U > U^*$. Figure 11 shows the layer magnetizations of the AFM1 solution ($\langle n\rangle = 0.3$, $T=0$). Apart from the first and the second layer, the magnetization of all layers are identical with the bulk sublattice magnetizations. Whether the calculation is performed including the crystal surface or not, does not affect the resulting bulk sublattice magnetizations.

Irrespective of the value for U we find the magnetization of the first layer to be larger than the corresponding bulk sublattice magnetization for the AFM1 solution. For the band filling $\langle n\rangle = 0.3$ this can be seen from Fig. 11. We have performed systematic investigations for the whole range of $\langle n\rangle$, which prove this to be a typical result: Provided that an antiferromagnetic solution is existing, the calculation yields an enhanced magnetization (absolute value) of the topmost surface layer with respect to the bulk for arbitrary Coulomb interaction U and arbitrary band filling $\langle n\rangle$. This holds true for all three types of antiferromagnetic configurations considered. No uniform behavior, however, could be found with respect to the magnetization of the second layer.

In the case of the ferromagnet, the situation is more complicated. The results presented in Fig. 9 are typical: For each band filling $\langle n\rangle$ there is a critical U above which ferromagnetic solutions are existing in the semi-infinite system. For all band fillings and for not too high values of U, the magnetization of the topmost surface layer is found to be larger than in the bulk. In Fig. 9 ($\langle n\rangle = 0.3$) this applies to all U ranging from $U/W = 1.04$, above which the surface layers order ferromagnetically, up to $U/W = 1.21$. At higher values the bulk magnetization and the magnetizations of all surface layers are almost saturated ($\langle n_{i\downarrow}\rangle \mapsto 0$), the saturation magnetization of the topmost surface layer $m_{\mathrm{sat}}^{(s)}$ being *smaller* than the bulk saturation magnetization $m_{\mathrm{sat}}^{(b)}$. The following general rule can be deduced from our calculations: $m_{\mathrm{sat}}^{(s)} \leq m_{\mathrm{sat}}^{(b)}$ for $\langle n\rangle \leq 0.5$, $m_{\mathrm{sat}}^{(s)} \geq m_{\mathrm{sat}}^{(b)}$ for $0.5 \leq \langle n\rangle \leq 1.5$, and $m_{\mathrm{sat}}^{(s)} \leq m_{\mathrm{sat}}^{(b)}$ for $1.5 \leq \langle n\rangle \leq 2.0$.

This rule for the saturation magnetization of the topmost layer at a ferromagnetic surface can be explained in a way analogous to the explanation of a similar rule that concerns the sign and magnitude of the shifts of the density of states at a paramagnetic surface with varying band filling (see e.g., Ref. 25): First, it is sufficient to consider a less than half-filled band only; due to the symmetry of the Bloch density of states the case $\langle n\rangle > 1.0$ is symmetric to the case $\langle n\rangle < 1.0$. Next, we may concentrate on the $\uparrow$ LDOS; in the case of ferromagnetic saturation and less than half-filled band the $\downarrow$ LDOS is unoccupied, and $\langle n\rangle = \langle n_\uparrow\rangle$, $\langle n_\downarrow\rangle = 0$. We note that the reduced coordination number of the surface atoms yields a narrowing of the $\uparrow$ LDOS of the topmost layer as discussed in Sec. V B. If layerwise charge neutrality is assumed for a moment, the band narrowing implies different Fermi energies for the bulk and the surface $\uparrow$ LDOS: For $\langle n_\uparrow\rangle < 0.5$ ($\langle n_\uparrow\rangle > 0.5$) the Fermi energy of the surface $\uparrow$ LDOS lies above (below) that of the bulk $\uparrow$ LDOS (for $\langle n_\uparrow\rangle = 0.5$ the Fermi energies coincide at the maximum of the surface $\uparrow$ LDOS). To restore equilibrium and thus coincidence of the Fermi levels, we have to allow for a small charge transfer. Consequently, the band narrowing finally results in $\langle n_\uparrow\rangle^{(s)} < \langle n_\uparrow\rangle^{(b)}$ ($\langle n_\uparrow\rangle^{(s)} > \langle n_\uparrow\rangle^{(b)}$) and therefore in a smaller (higher) saturation magnetization $m_{\mathrm{sat}}^{(s)} = \langle n_\uparrow\rangle^{(s)}$ of the topmost surface layer. Of course, in the self-consistent calculation a smaller (higher) filling of the surface $\uparrow$ LDOS in turn means a small shift of the center of gravity towards lower (higher) energies and thereby an increase (decrease) of $\langle n_\uparrow\rangle^{(s)}$. The requirement of self-consistency slightly reduces but does not reverse the effect. Finally, with respect to the magnetization of the second layer no similar rule could be found for the ferromagnet as in the case of the antiferromagnet.

D. Temperature dependence

In the case of bulk ferromagnetism the Stoner model predicts a rigid shift between the $\uparrow$ and the $\downarrow$ subband of $U \cdot m$. The exchange splitting is therefore temperature dependent. It typically amounts to several eV at $T=0$ and disappears for $T \geq T_C$. In Fig. 12 the result of a bulk calculation for $\langle n\rangle = 0.7$ and $U/W = 1.5$ is shown. At $T=0$ the magnetization is saturated, and the $\uparrow$ and the $\downarrow$ LDOS are energetically just separated from each other. Since the huge $T=0$ gap of $U \cdot m = U \cdot n = 12.6$ eV has to be closed at $T = T_C$, the

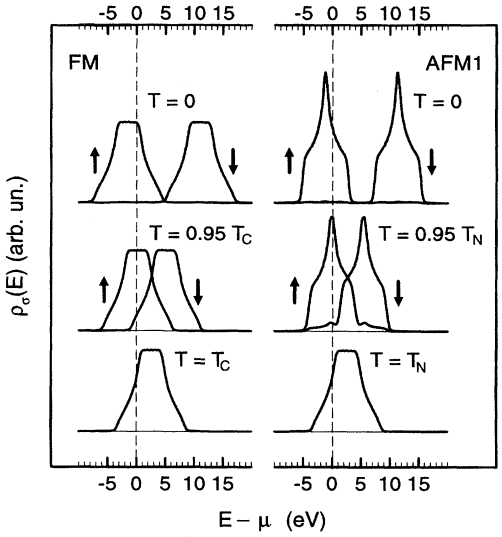

FIG. 12. Spin-dependent bulk LDOS at different temperatures for $\langle n\rangle = 0.7$ and $U/W = 1.5$. Calculation for the FM and the AFM1 structure. Temperatures given in units of the Curie temperature $T_C = 42\,900$ K and the Néel temperature $T_N = 43\,700$ K, respectively.

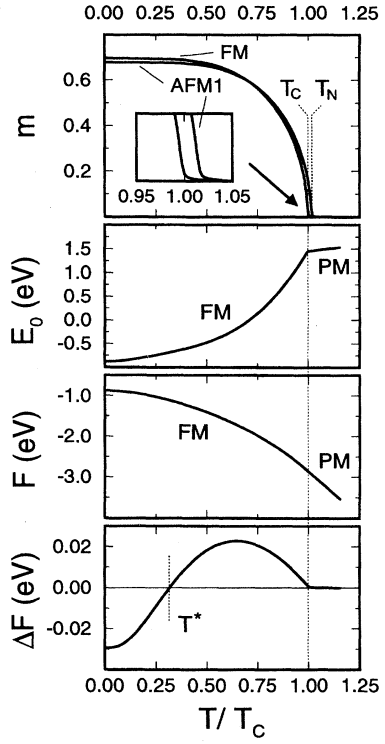

FIG. 13. Temperature dependence of the bulk (sublattice) magnetization m for the ferromagnetic (FM) and the AFM1 antiferromagnetic solution, the internal energy E_0 (for FM), the free energy F (for FM), and of the difference between the free energy for the FM and the free energy for the AFM1 solution ΔF. Bulk calculation for $\langle n\rangle = 0.7$ and $U/W = 1.5$.

Stoner model predicts a rather high Curie temperature of about $T_C = 42\,900$ K. For an antiferromagnet of AFM1 type and otherwise unchanged parameters, the Stoner model yields a Néel temperature in the same order of magnitude: $T_N = 43\,700$ K. The mechanism, however, that leads to decreasing magnetization with increasing temperature is completely different for the different magnetic structures (see Fig. 12). While for the ferromagnet there is an increasing overlap of the ↑ and the ↓ LDOS for $T \mapsto T_C$, it is a proper deformation of the LDOS that reduces the sublattice magnetization in the case of an antiferromagnet.

The Stoner model may reproduce the ground-state properties rather well, the unrealistic critical temperatures, however, indicate that it is overcharged to describe the correct temperature dependence of band magnets. We have to bear in mind this fact when investigating the temperature dependence of the magnetization at the very surface. Within the mean-field approach we can only get a first insight into temperature-dependent surface magnetism.

Figure 13 (first from top) shows the bulk (sublattice) magnetization as a function of temperature for the ferromagnetic as well as for the AFM1 antiferromagnetic solution ($\langle n\rangle = 0.7$, $U/W = 1.5$). For both, the temperature dependence is Brillouin-functionlike. This implies a second-order phase transition at T_C or T_N, respectively. The second panel shows the temperature dependence of the internal energy E_0 for the case of the ferromagnet. At $T = T_C$ the internal energy shows up a noncontinuous derivative. The free energy F that is decisive for the stability of solutions in the case $T \neq 0$, is a concave function of temperature with a continuous derivative at $T = T_C$ [cf. Eq. (10)]. Finally, the fourth panel shows the difference ΔF between the free energy of the ferromagnetic and the free energy of the antiferromagnetic solution. The bulk calculation shows the ferromagnetic solution to be stable at $T = 0$ ($\Delta F < 0$). At $T = T^*$ there is a first-order transition from the ferromagnetic to the antiferromagnetic phase until at $T = T_N$ the system undergoes a second-order transition to the paramagnetic state. Metastable ferromagnetic solutions exist for all temperatures between $T = T^*$ and $T = T_C$.

We now turn to the results of calculations that explicitly take into account the crystal surface. Figure 14 shows the temperature dependence of the magnetization for the first eight surface layers ($\langle n\rangle = 0.7$, $U/W = 1.5$). At $T = 0$ a ferromagnetic solution exists: The magnetizations of all surface layers are nearly identical to the bulk magnetization except for the magnetization of the topmost surface layer, which is slightly enhanced. According to the discussion above, the ferromagnetic solution is stable against the additionally existing AFM1 antiferromagnetic solution at $T = 0$. Between $T = 0$ and $T = T^*$ there is a stable ferromagnetic state. Provided that the temperature is increased "slowly" from $T < T^*$ to $T > T^*$, the system will remain ferromagnetic. A metastable ferromagnetic solution is found for temperatures above T^* up to a critical temperature of about $0.981\ T_C$. In contrast to the bulk calculation, no ferromagnetic solutions exist at higher temperatures, and the system is forced into the stable AFM1 antiferromagnetic state. The metastable ferro-

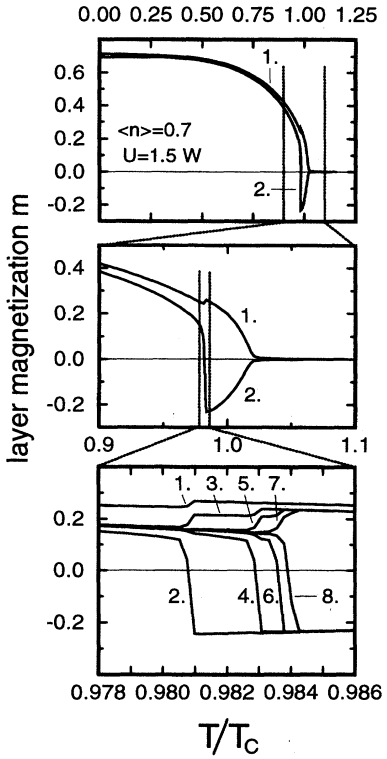

FIG. 14. Magnetizations of the first eight layers below the surface as functions of temperature for $\langle n\rangle = 0.7$ and $U/W = 1.5$. Calculation starting from ferromagnetic order at $T = 0$ (see text). Note the different temperature scales. Parameters: $L = 15$, $R = 10a$, $\Gamma = W/100$, and $\alpha = W/20$.

magnetic state is destroyed due to the presence of the surface, which acts as a perturbation of the periodic lattice. This interpretation is corroborated by the observation that the transition from the ferromagnetic to the antiferromagnetic phase starts from the very surface: At $T \approx 0.981 T_C$ the magnetization of the second layer switches its sign, at $T \approx 0.983 T_C$ the fourth layer, at $T \approx 0.984 T_C$ the sixth layer, and so on. The antiferromagnetic ordering of the layer magnetizations quickly penetrates into the crystal volume. The transition is completed at about $0.985 T_C$. For higher temperatures the antiferromagnetic order extends over the whole bulk.

Starting with the antiferromagnetic solution and decreasing the temperature from $T < T_N$ to $T = 0$ does not lead to an analogous effect: Metastable antiferromagnetic solutions are found for all temperatures below $T = T^*$. Concludingly, there is a surface-induced phase transition with increasing temperature T, which is qualitatively similar to the one found for decreasing Coulomb interaction U (Sec. V C).

VI. SUMMARY

We have investigated local magnetic properties at the surface of a band magnet within the framework of the semi-infinite Hubbard model. The (100) surface of a simple cubic crystal considered in the present study has served as a model system to show up the general trends and to look for qualitative new effects.

The absence of some nearest neighbors of atoms at the very surface causes considerable changes in the surface density of states. The deviations from the bulk density of states are confined to the first few surface layers. Integral quantities, such as the layer-dependent charge density and magnetization, mostly approach their bulk values already at the third or fourth layer below the surface. There is one exception to this rule, namely a metastable state with ferromagnetic order in the bulk and antiferromagnetic order that has been observed to extend over the first eight layers below the surface and more. However, such states have been found to exist in a very restricted parameter range only, as discussed in Secs. V C and V D.

For a given spin direction the surface and the bulk LDOS always share common band edges; no split-off states have been found in this study for the ferromagnetic as well as for all antiferromagnetic phases that have been considered. For the ferromagnetic solutions this implies that any deviation of the layer magnetization at the surface from its bulk value is due to a density-of-states effect and not due to an additional Stoner-like shift of the spin-dependent subbands.

In the case of antiferromagnetic structures, the narrowing of the LDOS gives rise to an always enhanced sublattice magnetization of the topmost layer. Contrary, for the ferromagnetic structure a larger magnetization of the topmost layer has only been found for not too strong Coulomb interaction. Whether the saturation magnetization of the topmost layer is smaller or larger than in the bulk, depends on the charge transfer between the bulk and the surface, which in turn is caused by the narrowing of the LDOS of the topmost layer. We could argue that for a band filling $0.5 \leq \langle n\rangle \leq 1.5$ the saturation magnetization of the topmost layer is enlarged and otherwise reduced with respect to the bulk. Depending on U, $\langle n\rangle$, and T, there may be a considerable change in the magnetization at the very surface for all magnetic structures, while there is hardly any charge transfer.

The perturbation of the infinitely extended periodic lattice due to the presence of the crystal surface has been found to be decisive for the existence of a metastable ferromagnetic state. Under certain conditions concerning the Coulomb interaction, the band filling, and the temperature, the perturbation can be strong enough to force the system into a stable layerwise antiferromagnetic state. This interpretation is corroborated by the observation that the antiferromagnetic order is not established instantaneously but starts from the very surface and then quickly extends into the bulk layer by layer.

The Hubbard model for the semi-infinite crystal represents an important starting point for the investigation of itinerant surface magnetism. Within its framework the complex interplay between lattice structure, surface geometry, Coulomb interaction, band filling, and temperature can be analyzed. To deal with real metal surfaces, the model has to be extended to include effects due to band degeneracy and hybridization, for example. Moreover, at the very surface different values for the hopping integrals and the Coulomb interaction should be taken into account. The most serious

shortcoming of the present study, however, is the mean-field approximation that has been applied to solve the many-body problem. This rather simple treatment of electron correlations can only provide a first insight into the problem, especially as the temperature dependence is concerned. We have thus focused only on general trends so far. To proceed to a more quantitative theory we aim at an improved description of electron-correlation effects that is clearly beyond the mean-field approach. Such work is in progress and will be the subject of a forthcoming paper.

ACKNOWLEDGMENTS

This work was funded by the Deutsche Forschungsgemeinschaft within the Sonderforschungsbereich 290.

[1] M. Lannoo and P. Friedel, *Atomic and Electronic Structure of Surfaces* (Springer, Berlin, 1991).
[2] R. Allenspach, J. Magn. Magn. Mater. **129**, 160 (1994).
[3] H. Krakauer, A. J. Freeman, and E. Wimmer, Phys. Rev. B **28**, 610 (1983).
[4] S. Ohnishi, A. J. Freeman, and M. Weinert, Phys. Rev. B **28**, 6741 (1983).
[5] C. L. Fu and A. J. Freeman, Phys. Rev. B **33**, 1755 (1986).
[6] J. Tersoff and L. M. Falicov, Phys. Rev. B **26**, 6186 (1982).
[7] R. H. Victora, L. M. Falicov, and S. Ishida, Phys. Rev. B **30**, 3896 (1984).
[8] R. H. Victora and L. M. Falicov, Phys. Rev. B **31**, 7335 (1985).
[9] J. Dorantes-Dávila, A. Mokrani, A. Vega, A. Rubio, C. Demangeat, H. Dreyssé, and L. C. Balbás, Surf. Sci. **251/252**, 51 (1991).
[10] A. Vega, L. C. Balbás, J. Dorantes-Dávila, and G. M. Pastor, Surf. Sci. **251/252**, 55 (1991).
[11] W. Nolting and W. Borgieł, Phys. Rev. B **39**, 6962 (1989).
[12] S. Bei der Kellen, W. Nolting, and G. Borstel, Phys. Rev. B **42**, 447 (1990).
[13] J. Hubbard, Proc. R. Soc. London, Ser. A **276**, 238 (1963).
[14] M. C. Gutzwiller, Phys. Rev. Lett. **10**, 159 (1963).
[15] J. Kanamori, Prog. Theor. Phys. (Kyoto) **30**, 275 (1963).
[16] R. Haydock, in *Solid State Physics: Advances in Research and Applications,* edited by H. Ehrenreich, F. Seitz, and D. Turnbull (Academic, New York, 1980), Vol. 35.
[17] *The Recursion Method and Its Applications*, Springer Series in Solid State Sciences, Vol. 58, edited by D. G. Pettifor and D. L. Weaire (Springer, Berlin, 1984).
[18] R. J. Jelitto, J. Phys. Chem. Solids **30**, 609 (1969).
[19] P. Turchi, F. Ducastelle, and G. Tréglia, J. Phys. C **15**, 2891 (1982).
[20] For acceleration of numerical convergence to self-consistency a modified version of Broyden's scheme has been applied, see, G. P. Srivastava, J. Phys. A **17**, L317 (1984).
[21] This seems to be in contrast to the results of Ref. 11 where AFM solutions have been found for $\langle n\rangle = 1.0$ and $U = 0^+$. That work, however, was based on a quite different Bloch density of states.
[22] P. W. Anderson, in *Solid State Physics: Advances in Research and Applications,* edited by F. Seitz and D. Turnbull (Academic, New York, 1963), Vol. 14, p. 99.
[23] G. Bulk and R. J. Jelitto, Phys. Rev. B **41**, 413 (1990).
[24] For the special case $U = 0$ our results become identical with the calculations of Haydock and Kelly [R. Haydock and M. J. Kelly, Surf. Sci. **38**, 139 (1973)].
[25] P. H. Citrin and G. K. Wertheim, Phys. Rev. B **27**, 3176 (1983).